Method for full Bloch sphere control of a localized spin via a single electrical gate

Joseph Pingenot, Craig E. Pryor, and Michael E. Flatté[a)]

Optical Science and Technology Center and Department of Physics and Astronomy, University of Iowa, Iowa City, Iowa 52242, USA

We calculate the dependence on an applied electric field of the **g** tensor of a single electron in a self-assembled InAs/GaAs quantum dot. We identify dot sizes and shapes for which one in-plane component of the **g** tensor changes sign for realistic electric fields, and show that this should permit full Bloch sphere control of the electron spin in the quantum dot using only a static magnetic field and a single vertical electric gate. © 2008 American Institute of Physics. [DOI: 10.1063/1.2937305]

Manipulating individual spins in solids requires quickly and coherently reorienting localized spins while leaving neighboring spins unaffected.[1] Difficulties confining oscillating magnetic fields have motivated alternate approaches that use electric fields to change the local magnetic environment, including moving an electron within a hyperfine field gradient[2] or fringe-field gradient.[3] Higher temperatures require spins to be localized in much smaller quantum dots (QDs), where these techniques are less effective. In contrast, approaches that couple the spin to an electric field via the spin-orbit interaction,[4–11] especially via **g** tensor manipulation techniques,[9] should be scalable to small dots with large confinement. Here, we calculate the **g** tensor of a single electron in a small QD and show that the symmetry of its electric field dependence permits full Bloch sphere control of the spin using an electric field applied in a single direction. We find the spin manipulation frequency of an InAs/GaAs QD in 1 T exceeds 150 MHz.

The energy difference between a spin-up and spin-down state (Zeeman energy) of an electron in a zinc blende direct-gap semiconductor depends on the band gap and spin-orbit splitting in the material.[12] The Zeeman energy thus can be modulated in a semiconductor heterostructure, even for a static magnetic field, by changing the overlap of the electronic wave function with different materials.[6–8,10] Other contributions in a system of low symmetry, such as a quantum well or QD, produce very different Zeeman energies from the same magnetic field when it is applied along different principal axes,[13] as described by the Hamiltonian

$$H = -\frac{e}{2m_e}\mathbf{S}\cdot\mathbf{g}\cdot\mathbf{B} = \mathbf{S}\cdot\mathbf{\Omega}. \tag{1}$$

Here, e is the electron charge, m_e is its mass, **S** is the electron spin operator, g is the Landé **g** tensor, **B** is the magnetic field, $\hbar$ is Planck's constant, and **Ω** is the spin precession vector. From Eq. (1), a change in the Zeeman energy in a static magnetic field corresponds to a change in the **g** tensor. As the **g** tensor changes due to a changing applied electric field in a semiconductor heterostructure, the spin precession vector **Ω** changes both its magnitude and direction, permitting reorientation of the spin. An oscillating electric field produces an oscillating transverse **Ω**, which allows resonant control of the spin orientation in a static magnetic field, as demonstrated in quantum wells.[9] As these manipulations only require electric field modulation, traditional high-density electric gate design strategies may be applicable to high-density arrays of single-spin devices.

Several significant challenges stand in the way of manipulating single spins using these methods. The strong confinement in QDs leads to a quenching of the orbital motion of the electron, driving the components of the **g** tensor toward the free-electron value of 2, and reducing the modulation of the **g** tensor in an electric field.[14] The long spin coherence times for electrons relative to holes[2,15,16] favors their use as coherent single-spin entities. To be able to conveniently and rapidly reorient the spin to any direction on the Bloch sphere, the ability to generate precession around two orthogonal axes is highly desirable, which might be expected to involve independent control of two electric fields. Manipulating an electric field along two directions in a nanoscale device would make the high-density integration of single-spin devices considerably more complex. We find that tall dots provide sufficient tuning for 150 MHz spin manipulation and that full Bloch sphere control is possible with a single vertical gate.

We now consider a single electron in an InAs/GaAs dot in a static magnetic field, with a series of electric fields applied by a top gate which will reorient the spin in an arbitrary direction (Fig. 1). The growth direction is [001] and the principal axes of the **g** tensor are [001], [110], and [1$\bar{1}$0]. We will refer to the values of **g** along these principal axes as the **g** tensor components. The magnetic field lies in the [001]-[110] plane, for reasons described later. The initial field E_1 gives an $\mathbf{\Omega}(E_1)$ parallel to [001] [Fig. 1(a)], allowing efficient spin initialization by optical illumination[15,17] and stabilizing the spin polarization until it is time to manipulate the spin. Guaranteeing this orientation of $\mathbf{\Omega}(E_1)$ for the magnetic field in Fig. 1 requires $g_{[110]}(E_1)=0$ and $g_{[001]}(E_1)\neq 0$ (here, assumed <0). Figures 1(b) and 1(c) show the QD's spin dynamics in response to the electric fields E_2 and E_3, which produce spin precession vectors along two perpendicular axes. Figure 1(d) returns the electric field to E_1. The polarization of the single spin along [001] can now be measured optically, e.g., by the Faraday or Kerr rotation.[18,19]

The two perpendicular spin precession vectors shown in Figs. 1(b) and 1(c) are central to achieving full Bloch sphere control of the spin. This condition is $\mathbf{\Omega}(E_2)\cdot\mathbf{\Omega}(E_3)=0$, which can be rewritten using Eq. (1) as
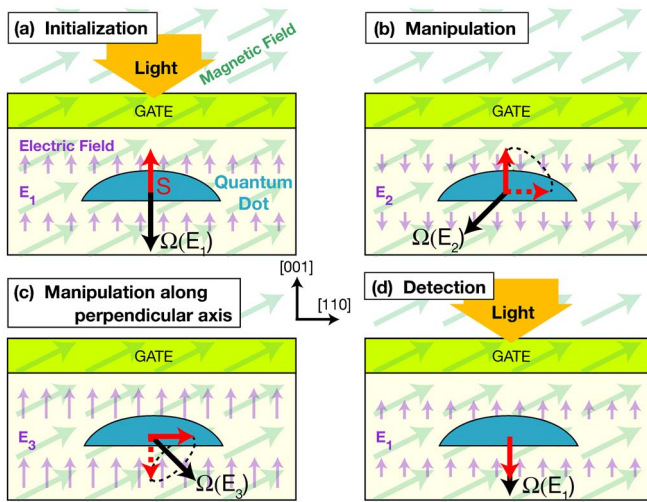
a)Electronic mail: michael-flatte@uiowa.edu.

FIG. 1. (Color online) Sequence of applied electric fields for injection, manipulation, and detection of an electron spin in a single QD. (a) for electric field E_1 the spin precession axis $\mathbf{\Omega}(E_1)$ is parallel to [001], easing optical spin injection. (b) For electric field E_2, the spin precession axis $\mathbf{\Omega}(E_2)$ rotates 45° toward the [110] direction. (c) For electric field E_3, the spin precession axis $\mathbf{\Omega}(E_3)$ is perpendicular to $\mathbf{\Omega}(E_2)$. (d) Return to an electric field E_1 eases optical measurement of the spin polarization along the [001] direction.

$$0 = g_{[001]}(E_2)g_{[001]}(E_3)B^2_{[001]} + g_{[110]}(E_2)g_{[110]}(E_3)B^2_{[110]}, \quad (2)$$

for $B_{[1\bar{1}0]}=0$. Equation (2) can only be satisfied if one (and only one) of the **g** components changes sign, which should be $g_{[110]}$ to permit the desired configuration in Fig. 1(a). A change in sign for a component of **g** has been demonstrated experimentally in quantum wells[8] but the observed changes of **g** in QDs have been very small.[11] A change in sign with *magnetic* field has been predicted theoretically for large QDs.[20] Here, we rely on a change in electric field to change the sign, which is suggested by the height dependence of the in-plane components of the **g** tensor.[14] This effect was also hinted at by the difference in sign between growth-direction **g** tensor components calculated for spherical and semispherical CdTe dots.[21] Thus, to achieve full control over a spin with only a single, growth-direction electric field, as shown in Figs. 1(b) and 1(c), one component of the **g** tensor must change sign. That component would be preferably along an axis perpendicular to the growth direction.

We now describe our calculated results of **g** for a broad range of InAs/GaAs QDs, and find many dots for which one in-plane component of the **g** tensor changes sign with applied electric field. Our evaluation of the precession frequency of the spin in these dots under the conditions of Figs. 1(b) and 1(c) yields ~150 MHz in a 1 T field. The precession frequency scales with the magnitude of the applied magnetic field, so a reasonable laboratory field can produce a precession frequency in excess of 1 GHz.

We calculate the electron **g** tensor in the dots using a strain-dependent eight-band **k·p** model[22] solved in real space[23] that includes both the orbital and the spin effects of the magnetic field in a lattice gauge theory formulation.[14] To calculate a **g** tensor component along a principal axis ([001], [110], or [1$\bar{1}$0]), a 1 T field is applied along the corresponding axis and the energy splitting between the two lowest-energy spin-dependent conduction states is determined. The
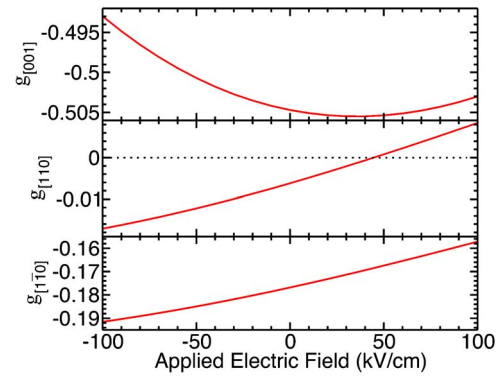

FIG. 2. (Color online) **g** tensor components of a QD as a function of an applied electric field along the [001] direction. The lens-shaped QD has a height of 6.2 nm, base diameter in the [110] direction of 15.6 nm, and base diameter in the [1$\bar{1}$0] direction of 9.2 nm. $g_{[110]}$ crosses from negative to positive near 50 kV/cm.

sign of each **g** tensor component was found by computing $\langle\psi|\mathbf{S}\cdot\hat{B}|\psi\rangle$ to determine the spin alignment.

The electric field dependence of the **g** tensor components is shown in Fig. 2 for a dot with a geometry favorable for spin manipulation for the magnetic field shown in Fig. 1. The lens-shaped dot has a height of 6.2 nm, with a base elongated along the [110] direction so that the dot diameters in the in-plane directions differ: $d_{[110]}$=15.6 nm and $d_{[1\bar{1}0]}$=9.2 nm. Dot height-to-base aspect ratios and elongations such as this can be achieved by manipulating growth conditions. Even larger height-to-base aspect ratios are possible using pillaring techniques.[24] A key feature of this dot is that $g_{[110]}$=0 for an electric field (~50 kV/cm) considerably below the breakdown voltage of the host semiconductor (>200 kV/cm). As the dot shape is not symmetrical along the [001] direction, the response to the electric field is not symmetric around E=0 and has a sizable E-linear dependence. This effect will occur for all asymmetric dots, including lithographic dots, but to a different degree. All electric fields considered in Fig. 2 are less than half the typical breakdown field of GaAs. The sign of all the **g** tensor components is negative at E=0. We can select from Fig. 2 the values of the electric field that correspond to the panels in Fig. 1. Figures 1(a) and 1(d) correspond to E_1=50 kV/cm, for which $g_{[110]}$=0 and Ω is parallel to [001]. Figure 1(b) corresponds to E_2=−50 kV/cm, for which $g_{[110]}$=−0.01. Figure 1(c) corresponds to E_3=100 kV/cm, for which $g_{[110]}$=+0.01. For a magnetic field rotated slightly (3.4°) from [110] toward the [001] direction, the spin precession axis will point, as shown in Figs. 1(b) and 1(c) for E_2 and E_3.

Figure 3 shows the results of a more extensive study as a function of dot shape and size. For E=0 the trends in **g** are similar to those reported earlier for both growth direction[14,25] and in-plane components.[14] In Fig. 3(a), the dot footprint is fixed and the height is changed. The results are plotted as a function of QD energy gap. Figure 3(b) shows similar results but the height is fixed and the footprint is changed. The width of the bands corresponds to the change in **g** as the electric field is changed from −100 to 100 kV/cm. As shown in Fig. 3(a), for all three elongations ($=d_{[110]}/d_{[1\bar{1}0]}$), there is a height, corresponding to a QD energy gap of ~1.14 eV, for which $g_{[110]}$ will change sign with applied electric field. As shown in Fig. 3(b), however, for fixed height and varying
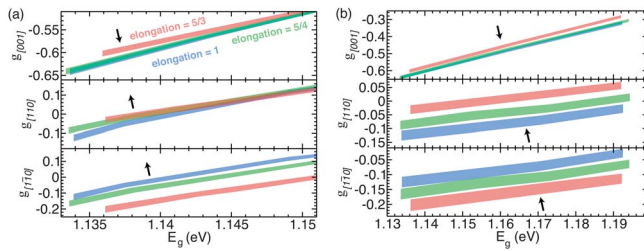
FIG. 3. (Color online) **g** tensor components for dots of different shapes and sizes, plotted as a function of the resulting energy gap of the dot. Each band corresponds to a fixed footprint shape, characterized by the elongation ($=d_{[110]}/d_{[1\bar{1}0]}$). (a) Height is varied for elongations of $5/3$, $5/4$, and 1, with a fixed footprint, corresponding to a 13 nm geometric mean of $d_{[110]}$ and $d_{[1\bar{1}0]}$. (b) Footprint size is varied, with height fixed at 6.2 nm. The shades indicate the elongation of the dot. Application of an electric field (from -100 to $+100$ kV/cm) modifies the g factors within the color bands. The change within the band as the electric field is increased is indicated by the arrow in each panel.

footprint, $g_{[110]}$ will change sign with applied electric field for dots with gaps that vary by over 50 meV, permitting tuning of the optical excitation energy of an optimized dot.

In all cases, the smaller dots have larger QD energy gaps, due to the increased confinement of both electrons and holes. Increased electron confinement quenches the orbital angular momentum of the electronic wavefunction[14] and drives the **g** tensor closer to the free-electron value of 2. Thus, dots with larger E_g's will have **g** tensors closer to 2, a trend visible in Fig. 3. A positive electric field (E_1 and E_3 in Fig. 1) pushes the electronic wave function toward the base of the dot, whereas a negative electric field (E_2 in Fig. 1) pushes it toward the apex. The electric field dependence of the **g** tensor comes from several effects: confinement-induced angular momentum quenching,[14] changes in the dot energy gap due to the quantum confined Stark effect,[26] and variation in the heavy/light hole spitting from the electron wave function overlapping different parts of the inhomogeneously strained dot. These effects, along with the anisotropy of the dot confining potential, produce anisotropy in the electric field dependence of the **g** tensor that is even more extreme than the anisotropy in the magnitude of **g**.

We also find that dots with **g** tensor components that change sign are well suited for resonant oscillation of the **g** tensor (**g** tensor modulation resonance[9]). Here, the approach would be to use a static electric field and add a harmonically oscillating electric field. We linearize the field dependence of the components of the **g** tensor

$$g_i(t) = g_{i0} + \frac{\partial g_i}{\partial E} E \cos(\omega t), \tag{3}$$

and the resulting precession axis

$$\mathbf{\Omega}(t) = \mathbf{\Omega}_0 + \cos(\omega t)\mathbf{\Omega_t}. \tag{4}$$

The optimal choice of magnetic field orientation for resonant manipulation corresponds to maximizing the component of $\mathbf{\Omega}_t$ transverse to $\mathbf{\Omega}_0$. The Rabi frequency is

$$\Omega_{\text{Rabi}} = \frac{\mu_B |\mathbf{\Omega}_t|}{4\hbar}\left[1 - (\hat{\Omega}_t \cdot \hat{\Omega}_0)^2\right]^{1/2}. \tag{5}$$

To evaluate the Rabi frequency, we neglect the dependence of $g_{[001]}$ on electric field over the range shown in Fig. 2, as that dependence is much smaller than the relative changes of

the in-plane components. We find that the largest Rabi frequencies can be achieved for any in-plane orientation of the magnetic field if the proper polar angle (measured from [001]) for **B** is chosen. For the dot characterized in Fig. 2, the optimal polar angle ranges from $\pi/2$ for an in-plane magnetic field parallel to [110] to $\approx \pi/2 \pm \pi/6$ for an in-plane magnetic field parallel to $[1\bar{1}0]$. The resulting Rabi frequency is approximately 150 MHz for a 1 T magnetic field, essentially the same as the spin precession frequency obtained for the geometry shown in Figs. 1(b) and 1(c). Thus, for a reasonable laboratory magnetic field of 10 T, the Rabi frequency would exceed 1 GHz.

Full control of a localized spin using a single growth-direction electric field applied using a nanoscale top gate should provide scalable methods of manipulating single spins in semiconductor QD systems. The ability to set the electric field to make $g_{[110]}$ vanish also allows the spin precession vector to be oriented parallel to the growth direction when desired, and permits the convenient storage of optically excited polarized spins until they are ready for manipulation.

[1] *Semiconductor Spintronics and Quantum Computation*, edited by D. D. Awschalom, N. Samarth, and D. Loss (Springer, Heidelberg, 2002).
[2] J. R. Petta, A. C. Johnson, J. M. Taylor, E. A. Laird, A. Yacoby, M. D. Lukin, C. M. Marcus, M. P. Hanson, and A. C. Gossard, Science **309**, 2180 (2005).
[3] Y. Tokura, W. G. van der Wiel, T. Obata, and T. Tarucha, Phys. Rev. Lett. **96**, 047202 (2006).
[4] V. K. Kalevich and V. L. Korenev, JETP Lett. **57**, 571 (1993).
[5] M. Oestreich, S. Hallstein, and W. W. Rühle, IEEE J. Quantum Electron. **2**, 747 (1996).
[6] E. L. Ivchenko, A. A. Kiselev, and M. Willander, Solid State Commun. **102**, 375 (1997).
[7] H. W. Jiang and E. Yablonovitch, Phys. Rev. B **64**, 041307 (2001).
[8] G. Salis, Y. Kato, K. Ensslin, D. C. Driscoll, A. C. Gossard, and D. D. Awschalom, Nature (London) **414**, 619 (2001).
[9] Y. Kato, R. C. Myers, A. C. Gossard, J. Levy, and D. D. Awschalom, Science **299**, 1201 (2003).
[10] M. F. Doty, M. Scheibner, I. V. Ponomarev, E. A. Stinaff, A. S. Bracker, V. L. Korenev, T. L. Reinecke, and D. Gammon, Phys. Rev. Lett. **97**, 197202 (2006).
[11] T. Nakaoka, S. Tarucha, and Y. Arakawa, Phys. Rev. B **76**, 041301 (2007).
[12] L. M. Roth, B. Lax, and S. Zwerdling, Phys. Rev. **114**, 90 (1959).
[13] E. L. Ivchenko and G. E. Pikus, *Superlattices and Other Heterostructures* (Springer, New York, 1997).
[14] C. E. Pryor and M. E. Flatté, Appl. Phys. Lett. **88**, 233108 (2006).
[15] F. Meier and B. P. Zachachrenya, *Optical Orientation: Modern Problems in Condensed Matter Science* (North-Holland, Amsterdam, 1984), Vol. 8.
[16] M. Kroutvar, Y. Ducommun, D. Heiss, M. Bichler, D. Schuh, G. Abstreiter, and J. J. Finley, Nature (London) **432**, 81 (2004).
[17] C. E. Pryor and M. E. Flatté, Phys. Rev. Lett. **91**, 257901 (2003).
[18] M. N. Leuenberger, M. E. Flatté, and D. D. Awschalom, Phys. Rev. Lett. **94**, 107401 (2005).
[19] M. H. Mikkelsen, J. Berezovsky, N. G. Stoltz, L. A. Coldren, and D. D. Awschalom, Nat. Phys. **3**, 770 (2007).
[20] C. F. Destefani and S. E. Ulloa, Phys. Rev. B **71**, 161303 (2005).
[21] S. J. Prado, C. Trallero-Giner, A. M. Alcalde, V. López-Richard, and G. E. Marques, Phys. Rev. B **69**, 201310 (2004).
[22] T. B. Bahder, Phys. Rev. B **41**, 11992 (1990).
[23] C. Pryor, Phys. Rev. B **57**, 7190 (1998).
[24] J. He, H. Krenner, C. Pryor, J. P. Zhang, Y. Wu, D. Allen, C. Morris, M. Sherwin, and P. M. Petroff, Nano Lett. **7**, 802 (2007).
[25] T. Nakaoka, T. Saito, J. Tatebayashi, and Y. Arakawa, Phys. Rev. B **70**, 235337 (2004).
[26] S. A. Empedocles and M. G. Bawendi, Science **278**, 2114 (1997).